

$K^+\Lambda$ and $K^+\Sigma^0$ photoproduction with fine center-of-mass energy resolution

T.C. Jude*,¹ D.I. Glazier,¹ D.P. Watts†,¹ P. Aguar-Bartolome,² L.K. Akasoy,² J.R.M. Annand,³ H.J. Arends,² K. Bantawa,⁴ R. Beck,⁵ V.S. Bekrenev,⁶ H. Berghauser,⁷ A. Braghieri,⁸ D. Branford,¹ W.J. Briscoe,⁹ J. Brudvik,¹⁰ S. Cherepnaya,¹¹ B.T. Demissie,⁹ M. Dieterle,¹² E.J. Downie,^{2,9} L.V. Fil'kov,¹¹ R. Gregor,⁷ E. Heid,^{2,9} D. Hornidge,¹³ I. Jaegle,¹² O. Jahn,² V.L. Kashevarov,^{2,11} I. Keshelashvili,¹² R. Kondratiev,¹⁴ M. Korolija,¹⁵ A.A. Koulbardi,⁶ S.P. Kruglov,⁶ B. Krusche,¹² V. Lisin,¹⁴ K. Livingston,³ I.J.D. MacGregor,³ Y. Maghrbi,¹² D.M. Manley,⁴ Z. Marinides,⁹ T. Mart,¹⁶ M. Martinez,² J.C. McGeorge,³ E.F. McNicoll,³ D.G. Middleton,¹³ A. Mushkarenkov,⁸ B.M.K. Nefkens,¹⁰ A. Nikolaev,⁵ V.A. Nikonov,⁶ M. Oberle,¹² M. Ostrick,² P.B. Otte,² B. Oussena,^{2,9} P. Pedroni,⁸ F. Pheron,¹² A. Polonski,¹⁴ S. Prakhov,¹⁰ J. Robinson,³ G. Rosner,³ T. Rostomyan,^{8,12} A.V. Sarantsev,⁵ S. Schumann,² M.H. Sikora,¹ D.I. Sober,¹⁷ A. Starostin,¹⁰ I. Strakovsky,⁹ I.M. Suarez,¹⁰ I. Supek,¹⁵ M. Thiel,⁷ A. Thomas,² M. Unverzagt,² D. Werthmüller,¹² L. Witthauer,¹² and F. Zehr¹²

(The Crystal Ball at MAMI Collaboration)

¹*School of Physics, University of Edinburgh, Edinburgh EH9 3JZ, UK*

²*Institut für Kernphysik, University of Mainz, D-55099 Mainz, Germany*

³*Department of Physics and Astronomy, University of Glasgow, Glasgow G12 8QQ, UK*

⁴*Kent State University, Kent, Ohio 44242, USA*

⁵*Helmholtz-Institut für Strahlen- und Kernphysik, University of Bonn, D-53115 Bonn, Germany*

⁶*Petersburg Nuclear Physics Institute, 188300 Gatchina, Russia*

⁷*II Physikalisches Institut, University of Giessen, D-35392 Giessen, Germany*

⁸*INFN Sezione di Pavia, I-27100 Pavia, Italy*

⁹*The George Washington University, Washington, DC 20052, USA*

¹⁰*University of California Los Angeles, Los Angeles, California 90095-1547, USA*

¹¹*Lebedev Physical Institute, 119991 Moscow, Russia*

¹²*Institut für Physik, University of Basel, CH-4056 Basel, Switzerland*

¹³*Mount Allison University, Sackville, New Brunswick E4L3B5, Canada*

¹⁴*Institute for Nuclear Research, 125047 Moscow, Russia*

¹⁵*Rudjer Boskovic Institute, HR-10000 Zagreb, Croatia*

¹⁶*Departemen Fisika, FMIPA, Universitas Indonesia, Depok 16424, Indonesia*

¹⁷*The Catholic University of America, Washington, DC 20064, USA*

(Dated: June 10, 2022)

Precision measurements of $\gamma p \rightarrow K^+\Lambda$ and $\gamma p \rightarrow K^+\Sigma^0$ cross-sections have been obtained with the photon tagging facility and the Crystal Ball calorimeter at MAMI-C. The measurement uses a novel K^+ meson identification technique in which the weak decay products are characterized using the energy and timing characteristics of the energy deposit in the calorimeter, a method that has the potential to be applied at many other facilities. The fine centre-of-mass energy (W) resolution and statistical accuracy of the new data results in a major impact on partial wave analyses aiming to better establish the excitation spectrum of the nucleon. The new analyses disfavor a strong role for quark-diquark dynamics in the nucleon.

PACS numbers: 13.60.Le, 14.20.Gk, 25.20.Lj

Establishing the excitation spectrum of a composite system has historically been one of the most effective ways to determine the detailed nature of the interactions between its constituents. Establishing the excitation spectrum of the nucleon; a complex bound system of valence quarks, sea quarks and gluons, is currently one of the highest priority goals of hadron and nuclear physics. The spectrum is a fundamental constraint on our understanding of the nature of QCD confinement in light quark systems. Recent advances in theory have linked

the excitation spectrum to QCD via lattice predictions [1] and holographic dual theories [2]. These complement the phenomenological QCD-based models such as constituent quark models [3] and soliton models [4].

Despite its importance, the spectrum of nucleon resonances remains poorly established with the basic properties (electromagnetic couplings, masses, widths) and even the existence of many excited states uncertain (for a review see [5]). In an attempt to address this shortcoming, real photon beams have been used to excite nucleon targets, providing accurate data to constrain partial-wave analyses (PWA) and reaction models used to extract information on the excitation spectrum [6–11]. This is the choice method for such studies, as the photon probe has a well-understood interaction (QED) and polarization de-

*Present address: Physikalisches Institut, University of Bonn, Bonn 53115, Germany, jude@physik.uni-bonn.de

†dwatts1@ph.ed.ac.uk

degrees of freedom (linear and circular). A major program of measurements utilizing polarized photon beams, polarized targets and final-state nucleon polarimeters is currently underway with the goal to achieve a “complete”, model-independent measurement of photoproduction reactions.

The process $\gamma p \rightarrow K^+ \Lambda$ has the lowest energy threshold for photoproduction reactions with final-state particles containing strange valence quarks. This is a crucial channel as many models predict that some poorly established or “missing” resonances couple strongly to strange decay channels [12]. Isospin conservation demands that only N^* and not Δ resonances contribute to the reaction, simplifying the interpretation of the data. The weak decay of the Λ allows access to its polarization from the distribution of its decay particles and ensures that $\gamma p \rightarrow K^+ \Lambda$ will be the first photoproduction reaction measured with a complete set of experimental observables, providing a benchmark channel for PWAs.

Measurements of $\gamma p \rightarrow K^+ \Lambda$ from threshold, with sufficient statistics to resolve resonance structure, have been obtained with the SAPHIR [13, 14] and CLAS detectors [15, 16]. Unfortunately the cross-section data have discrepancies that lead to significant differences in the PWA solutions when using either data set (see [17] for a review), however, measurements of $\gamma p \rightarrow K^+ \Sigma^0$ with similar analysis procedures give closer agreement.

$\gamma p \rightarrow K^+ \Lambda$ data with fine center-of-mass energy (W) resolution would be an important constraint on the existence of narrow N^* states [18, 19]. A number of recent searches for narrow N^* near 1700 MeV were motivated by the prediction of a non-strange, nucleon-like, member of the anti-decuplet with strong photocoupling to the neutron [20]. In response to recent evidence, a speculative new N^* state at 1685 MeV was included in the recent Particle Data Group listings [21]. However, alternative explanations for the narrow structures are also offered based on interference structures arising from known resonances [22] or coupled-channel effects [23]. Disentangling the cause of the narrow structure in this mass region is likely to require accurate cross section and polarisation observables for a range of reaction channels.

The data presented here were taken with the Crystal Ball detector [24] at the Mainz Microtron accelerator facility (MAMI-C) [25] in a beamtime of 430 hours. The energy tagged photon beam of $\sim 10^5 \gamma \text{ MeV}^{-1} \text{ sec}^{-1}$ was produced by impinging the MAMI-C 1557.4 MeV electron beam on a thin copper radiator, with the photon energy (E_γ) determined by momentum analysis of the recoil bremsstrahlung electrons in the Glasgow Photon Tagger [26]. Photon energy resolutions in the range of 3 - 4 MeV were achieved, corresponding to resolutions in the centre of mass energy, W , in the range of 1.0 - 2.1 MeV. The photon beam was incident on a 10 cm long liquid hydrogen target comprising 4.2×10^{23} protons per cm^2 .

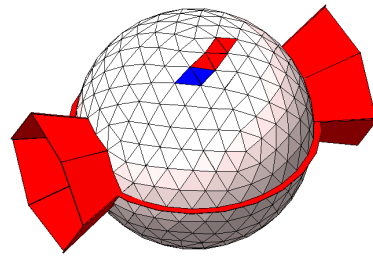


FIG. 1: (Color online) Visualization of the Crystal Ball in the Geant4 simulation. The shaded crystals have energy depositions following an incident K^+ . The blue and red show the IC and DC respectively (see text).

The Crystal Ball (Fig. 1) is a segmented calorimeter of 672 NaI crystals covering 94% of 4π steradians. Each crystal has separate TDC and ADC readouts giving a time resolution of 2 ns and a fractional energy resolution of $(1.7/E_\gamma)^{0.4}$ GeV. A Particle Identification Detector (PID), consisting of 24 plastic scintillators forming a cylinder [27], surrounded the target and gave an energy signal for charged particles.

Due to the comparatively high cross sections, contamination in the event sample from non-strange reaction channels prevented the extraction of $K^+ \Lambda$ and $K^+ \Sigma^0$ channels via conventional means. This work pioneers a new method of identifying K^+ in which its weak decay products are characterized by using the energy and timing characteristics of the detector hits in a segmented calorimeter. The weak decay can proceed via $K^+ \rightarrow \mu^+ \nu_\mu$ (muonic mode) or $K^+ \rightarrow \pi^+ \pi^0$ (pionic mode). The validity of the new technique was tested extensively by comparing a full Geant4 [28] simulation of the apparatus with the experimental data. The main results of these studies are presented in Fig. 2 and discussed below.

Each cluster of hit crystals produced from a charged particle event in the Crystal Ball was separated into two “sub-clusters”. The “incident-cluster” (IC) comprised those crystals having a timing coincidence within $\pm 3\sigma$ of the timing of the photoreaction in the target, where σ is the achievable coincidence timing resolution (~ 3 ns). Only events with summed IC energy ≥ 25 MeV and ≤ 2 crystals were retained. The crystals with coincidence time ≥ 10 ns later than the photoreaction were assumed part of the “decay-cluster” (DC) from the decay of the stopped K^+ . A minimum summed DC energy of 75 MeV and ≥ 4 crystals was required. A cluster pattern for a typical muonic decay event visualized in the Geant4 simulation is presented in Fig. 1.

Fig. 2(a) is the energy spectrum for the DC, exhibiting a peak at 150 MeV consistent with the energy of the muon in $K^+ \rightarrow \mu^+ \nu_\mu$ decay at rest. A shoulder extends to 350 MeV, which is the maximum energy deposition for the pionic decay ($K^+ \rightarrow \pi^+ \pi^0$). Fig. 2(b) is the time dif-

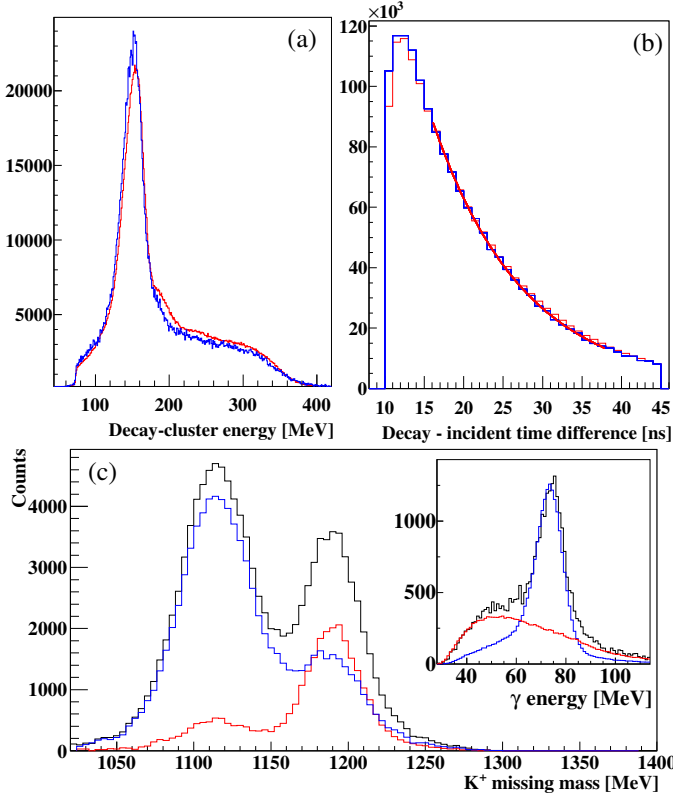


FIG. 2: (Color online) (a,b) Decay-cluster characteristics for experimental and simulated data (blue and red respectively): (a) DC summed energy, description in the text. (b) Time difference between IC and DC. (c) Missing (hyperon) mass for all K^+ detection (black), when the decay γ from $\Sigma^0 \rightarrow \gamma\Lambda$ is not identified (blue) and is identified (red). Inset: γ energy in the hyperon rest frame for experimental data (black), simulated $K^+\Lambda$ data (red) and simulated $K^+\Sigma^0$ data (blue).

ference between the IC and DC. An exponential fit gives a lifetime in agreement with the accepted K^+ lifetime. Selections on the linearity and energy distribution in the DC were used select the dominant muonic decay events, which gave better K^+ momentum resolution compared to the pionic decay events. The IC summed energy was then utilised in a $\Delta E - E$ analysis and used to reconstruct the K^+ momentum.

Fig. 2(c) is the reconstructed missing-mass of the system recoiling from the K^+ , exhibiting peaks at the Λ and Σ^0 invariant masses. A new technique to cleanly separate $\gamma p \rightarrow K^+\Lambda$ and $K^+\Sigma^0$ was used, via the identification of the decay $\Sigma^0 \rightarrow \Lambda\gamma$ in the Crystal Ball. Fig. 2(c) (inset) is the energy of the decay photons boosted into the hyperon rest frame, with the expected peak at the Σ^0 - Λ mass difference of 77 MeV. Events with energies between 55-95 MeV were selected as $K^+\Sigma^0$ candidates. Simulated data were used to determine the decay γ detection efficiency (approximately 60%, varying slightly with E_γ). The $K^+\Lambda$ yield was obtained by subtracting the

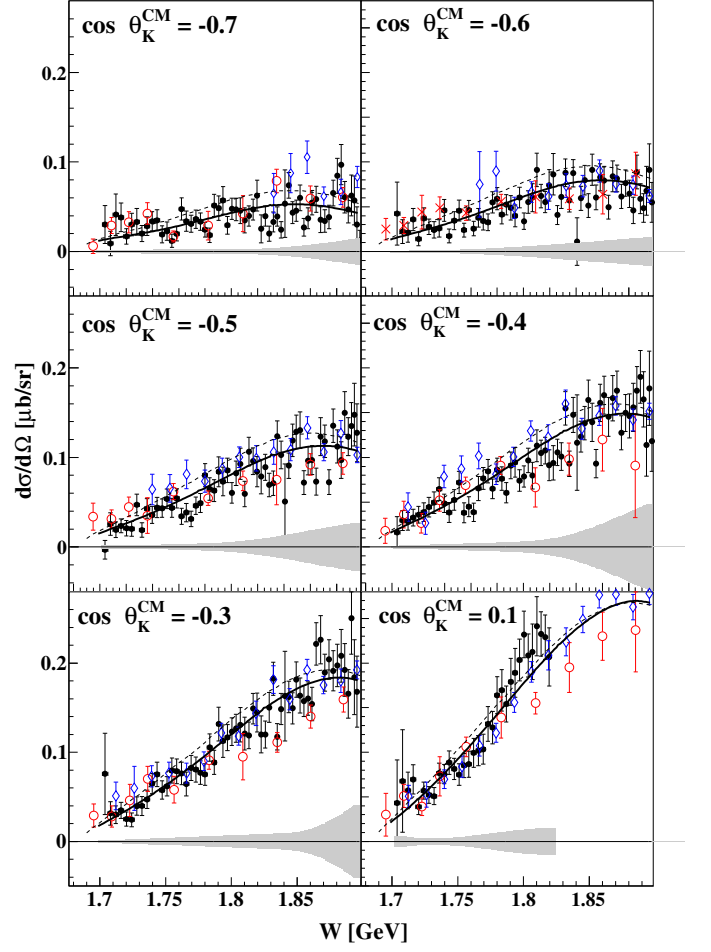


FIG. 3: (Color online) Differential $\gamma p \rightarrow K^+\Sigma^0$ cross-sections versus W . Black filled circles are the current data with systematic uncertainties plotted gray on the abscissa. Red open circles are SAPHIR data [13], blue open diamonds are CLAS data of Bradford *et al.* [15]. The dashed black line is the current BnGa 2011-2 solution [11] and the thick solid black line is the BnGa 2011-02 solution including the new $K^+\Lambda$ and $K^+\Sigma^0$ data [30]. (The SAPHIR data have $\cos \theta_K^{\text{CM}}$ intervals backwards by 0.05 than the given values.)

efficiency corrected yield of $K^+\Sigma^0$ candidate events from the missing mass spectra. This procedure gave a clean $K^+\Lambda$ invariant mass peak with negligible background. The small fraction (less than 5%) of $K^+\Lambda$ events which are misidentified in the $K^+\Sigma^0$ yield are accounted for in the calculated detection efficiency. A second method of fitting Gaussian functions to the total missing-mass spectra to separate the reaction channels gave an agreement with the above method to better than 4%, which is taken as the estimated systematic error.

Detection efficiencies were obtained by analyzing Geant4-simulated $K^+\Lambda$ and $K^+\Sigma^0$ events including appropriate timing and energy resolutions. Experimental trigger conditions were implemented as described in [29].

A maximum detection efficiency of approximately 10% was achieved. Systematic errors arose from the modelling of the experimental trigger ($\leq 4\%$) and the modelling of K^+ hadronic interactions in the Crystal Ball ($\leq 4\%$), assessed from comparison of different physics models in the simulation. The contribution from background channels passing the selection cuts (dominantly $\gamma p \rightarrow p\pi^+\pi^-$) was typically $\leq 2\%$. Systematics from non-hydrogen components of the target cell, target cell length and PID efficiency were $\leq 1\%$.

The quality of the new data is illustrated in Figs. 3 and 4, where cross-sections for $K^+\Sigma^0$ and $K^+\Lambda$ as a function of W are shown for selected center-of-mass K^+ polar angle bins (θ_K^{CM}), compared with previous SAPHIR [13] and CLAS [15, 16] data. For clarity, the data are rebinned by a factor of two, however the attainable W resolution of the new data is a factor of 4 to 10 improvement over previous data. The new $\gamma p \rightarrow K^+\Sigma^0$ data (Fig. 3) are consistent with previous measurements, demonstrating that systematic errors for the new detection techniques are well understood.

The data are compared to predictions from PWAs in the Kaon Maid (KM) [8] and Bonn-Gatchina (BnGa) [10] framework, which are constrained by the various combinations of data sets indicated in the figure caption. The main quoted systematic error in extracting resonance properties in the BnGa PWA framework is the existence of two solutions (BG2011-01 and BG2011-02) which give a similarly low χ^2 when fitted to the world database. The solutions have different resonance contributions and helicity couplings (for a detailed description see [10]). The addition of the new $K^+\Sigma^0$ and $K^+\Lambda$ data resolve these solutions. Only BG2011-02 can fit the new data and the world dataset with a satisfactorily low χ^2 of 1.3 and 1.2 for $K^+\Sigma^0$ and $K^+\Lambda$ respectively [32]. The most significant difference between the solutions is that BG2011-2 supports the need for two P_{13} nucleon resonances close in mass: a $P_{13}(1900)$ and $P_{13}(1975)$. Despite constituent quark models (CQM) predicting the existence of two $3/2^+$ nucleon states in the region 1850-2000 MeV, it is difficult to explain two such states in the framework of a quark-diquark model or under the assumption of chiral symmetry restoration. The new experimental data therefore provide new constraints on the dynamics of quarks within the nucleon and resolves ambiguities in the helicity coupling of a number of resonances, including the $N(1880)\frac{1}{2}^+$ [10]. The well defined structure in the $K^+\Lambda$ cross section around 1670 MeV at backward K^+ angles provides valuable constraint on the existence and width of the disputed [33] $P_{11}(1710)$ resonance. To fit the structure a 30% reduction in the resonance width was necessary in the BnGa analysis. Interestingly this produces a width now consistent with the other sightings of this resonance [5].

The total cross section for $\gamma p \rightarrow K^+\Lambda$ has been debated in the literature where structure around

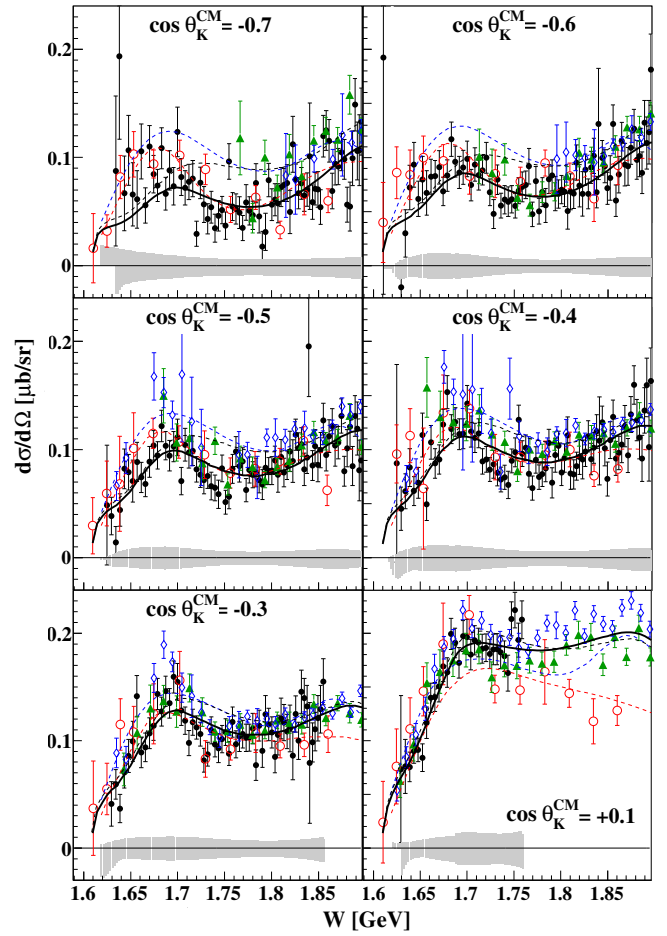


FIG. 4: (Color online) Differential $\gamma p \rightarrow K^+\Lambda$ cross-sections versus W . Data as described in Fig. 3, with additional CLAS data of McCracken *et al.* [16] (green filled triangles). Dashed red and blue lines are fits from the KM model to SAPHIR data and CLAS data [31] respectively.

$W \sim 1900$ MeV has been largely interpreted as evidence for a missing D_{13} resonance (for example [17] and references therein). Constraints from the new data lead to revised extrapolated total cross sections as shown in Fig. 5, where the KM and BnGa predictions now agree at the 10% level. The peak structure around $W \sim 1.9$ GeV is significantly suppressed with the inclusion of the new data.

The improvement in W resolution in the new data allows constraints on the existence of structures in the cross section arising from narrow resonance states or coupled channel effects. At backward angles, it is speculated that there is structure between 1650 - 1700 MeV not described by existing models. The new data has already been incorporated in a number of such studies and will be used in future publications.

In conclusion, new precision measurements of the $\gamma p \rightarrow K^+\Lambda$ and $\gamma p \rightarrow K^+\Sigma^0$ differential cross-section

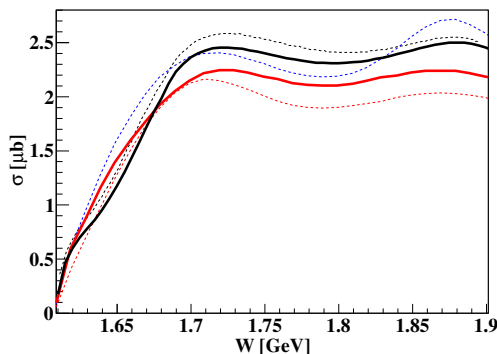


FIG. 5: Total $\gamma p \rightarrow K^+ \Lambda$ cross-section versus W from KM and BnGa solutions (the same line convention as in Fig. 3 with additional thick solid red line showing KM constrained by CLAS data and this current $K^+ \Lambda$ data [34]).

have been obtained with a novel new K^+ identification method. The new K^+ identification technique enables K^+ detection without the need for large scale spectrometers and has already been incorporated into the BGO-OD experiment [35] and will be the basis of an online K^+ trigger at MAMI, significantly increasing future K^+ yields. The technique is also a viable method for identifying K^+ in fast timing environments such as in plasma based accelerators. The new $\gamma p \rightarrow K^+ \Lambda$ and $\gamma p \rightarrow K^+ \Sigma^0$ data have significantly improved centre-of-mass energy resolution and statistical accuracy than previous data and provide a significant new constraint to the world database of meson photoproduction. A combined analysis of both reaction channels resolves the largest quoted systematic error in determining the resonance spectrum with the BnGa PWA framework, resulting in a preference for a nucleon resonance spectrum which is inconsistent with models assuming quark-diquark dynamics in the nucleon.

The authors acknowledge the excellent support of the MAMI-C accelerator group. This work was supported by the UK STFC, the German DFG (SFB 443), SFB/Tr16, the Schweizerischer Nationalfonds and the European Community-Research Infrastructure Activity under the FP6 “Structuring the European Research Area” program (HadronPhysics, Contact No. RII3-CT-2004-506078), DFG-RFBR (Grant No. 05-02-04014), the U.S DOE, U.S. NSF and NSERC (Canada).

[1] R.G. Edwards *et al.*, Phys. Rev. D **84**, 074508 (2011).

[2] S.J. Brodsky and G.F. de Teramond, Few-Body Syst. **52**,

203 (2012).

[3] S. Capstick and W. Roberts, Prog. Part. Nucl. Phys. **45**, s241 (2000).

[4] D. Diakonov and V. Petrov, World Scientific, **1**, 359 (2000), arxiv:hep-ph/0009006.

[5] E. Klempt and J.-M. Richard, Rev. Mod. Phys. **82**, 1095 (2010).

[6] T. Mart, Phys. Rev. C **62**, 038201 (2000).

[7] F.X. Lee, T. Mart, C. Bennhold, H. Haberzettl and L.E. Wright, Nucl. Phys. A **695**, 237 (2001).

[8] <http://www.kph.uni-mainz.de/MAID/kaon/kaonmaid.html>.

[9] R.A. Arndt, W.J. Briscoe, I.I. Strakovsky and R.L. Workman. SAID Partial-Wave Analysis Facility, gw-dac.phys.gwu.edu (2012).

[10] A.V. Anisovich *et al.*, Eur. Phys. J. A **47**, 153 (2011).

[11] A.V. Anisovich *et al.*, Eur. Phys. J. A **48**, 15 (2012).

[12] S. Capstick and W. Roberts, Phys. Rev. D **58**, 074011 (1998).

[13] K.H. Glander *et al.*, Eur. Phys. J. A **19**, 251 (2004).

[14] M.Q. Tran *et al.*, Phys. Lett. B **445**, 20 (1998).

[15] R. Bradford and R.A. Schumacher *et al.* (CLAS Collaboration), Phys. Rev. C **73**, 035202 (2006).

[16] M.E. McCracken, M. Bellis, C.A. Meyer, M. Williams *et al.*, Phys. Rev. C **81**, 025201 (2010).

[17] T. Mart, Int. J. Mod. Phys. E **19**, 2343 (2010).

[18] R.H. Arndt, Ya.I. Azimov, M.V. Polyakov, I.I. Strakovsky and R.L. Workman, Phys. Rev. C **69**, 035208 (2004).

[19] T. Mart, Phys. Rev. D **83**, 094015 (2011).

[20] V. Petrov, and M. V. Polyakov, Z Phys A **359**, 305 (1997)

[21] J. Beringer *et al.* (Particle Data Group), Phys. Rev. D **86**, 010001 (2012).

[22] V. Shklyar, H. Lenske and U. Mosel, Phys. Lett. B **650**, 172 (2007).

[23] M. Doring and K. Nakayama, Phys. Lett. B **683**, 145 (2010); A.V. Anisovich *et al.*, Phys. Lett. B **719**, 89 (2013).

[24] A. Starostin *et al.*, Phys. Rev. C **64**, 055205 (2001).

[25] K.-H. Kaiser *et al.*, Nucl. Instr. Meth. A **593**, 159 (2008).

[26] J.C. McGeorge *et al.*, Eur. Phys. J. A **37**, 129 (2008).

[27] D.P. Watts, *Proceedings of the 11th International Conference on Calorimetry in Particle Physics*, Perugia, Italy, World Scientific, 560 (2005).

[28] J. Allison *et al.*, IEEE Trans. on Nucl. Sci. **53**, 270 (2006).

[29] E.F. McNicoll, S. Prakhov and I.I. Strakovsky *et al.*, Phys. Rev. C **82**, 035208 (2010).

[30] A.V. Anisovich, private communication (2012).

[31] T. Mart and M.J. Kholili, Phys. Rev. C **86**, 022201 (2012).

[32] A.V. Sarantsev and V. Nikonov, private communication (2012).

[33] R. A. Arndt, W. J. Briscoe, I. I. Strakovsky, and R. L. Workman, Phys. Rev. C **79**, 065207 (2009).

[34] T. Mart, private communication (2012).

[35] H. Schmieden, Int. J. Mod. Phys. E, **19**, 1043 (2010).

[36] A. Martinez Torres *et al.*, Phys. Rev. C **74**, 045205 (2006).